

Fundamental study on simple quantitative approach of damping performance for semi-active damper



T. Hiwatashi

Toa Corporation, Yokohama, Japan

H. Fujitani

Kobe University, Kobe, Japan

SUMMARY:

Structural vibration control is categorized into passive control, active control and semi-active control. Semi-active control using a variable damper stabilizes building responses in an earthquake better than the conventional passive control and active control. This method aims to minimize a structure's response by changing the damper capacity according to the state of the structure and the external loads, and various kinds of semi-active control algorithms have been proposed. A lot of them utilize mathematically difficult algorithms that require complicated computer systems. With these methods, we can not evaluate the effectiveness and overall safety of the system under various kinds of loads. One reason is that the behaviors of structures incorporating such complicated control systems can not be evaluated by conventional means such as equivalent viscous damping factor based on hysteresis. Therefore, a semi-active control system is wished in which the control effects can be easily quantified as with passive control systems. This paper describes the result of having proposed the simple quantification approach for the semi-active control effectiveness.

Keywords: Structural vibration control, Variable hydraulic damper, Simple quantitative approach

1. INSTRUCTION

Using dampers is an effective method for reducing vibration of structures due to earthquake, strong wind, and traffic, thereby improving structural safety, comfort and functionality. As dampers can absorb and restrain vibration, this technique is particularly effective for skyscrapers, which are subject to strong vibration due to wind. The appropriate damping capacity for conventional dampers, which are passive-type, is determined based on the size of the target building and the estimated vibration magnitude. However, passive dampers have certain limits with their capability to control various types of unpredictable vibrations.

On the other hand, a semi-active control method can control the damping force of a semi-active damper, by taking in information such as ever-changing building responses and vibration. Therefore, semi-active dampers should be able to achieve a higher damping effect than passive dampers.

This paper proposes a method for evaluating the performance of a variable hydraulic damper, a type of semi-active damper, which is applied to a structure. This is a simple method for quantifying damping performance based on the amount of hysteresis energy by a damper that corresponds to the response of the structure. Using this quantitative evaluation method, the author considers it possible to evaluate the control effects of structures having different control laws, as well as the control effects of various semi-active dampers. This paper also verifies the quantitative evaluation approach by applying it to the results of a shaking table test.

2. PROPOSAL FOR A SIMPLIFIED QUANTIFICATION APPROACH

2.1. Evaluation of equivalent damping of stationary responses

As the actual damping of the building response is very complicated, it is often replaced with equivalent viscous damping. For example, an equivalent linearization method is used to evaluate the damping effects of elasto-plastic response by replacing it with equivalent period and equivalent damping. It is particularly effective when evaluating the damping effects of stationary responses and linear vibrations. For a stationary response, the equivalent viscous damping constant initially proposed by *Jacobsen* can be defined by the following equation, using the area represented by ΔW and W in Fig.1(a). Here, ΔW is loss of energy in one cycle, and W is elastic strain energy due to equivalent stiffness.

There is no problem in the case of stationary response. However, for the semi-active control, the hysteresis loop changes with the passage of time according to the control law. Thus, the evaluation of damping effects in semi-active control using the equivalent viscous constant may be considerably different from the actual damping effects (Fig.1(b)).

$$h_{eq} = \frac{1}{4} \left[\frac{\Delta W}{W} \right] \quad (2.1)$$

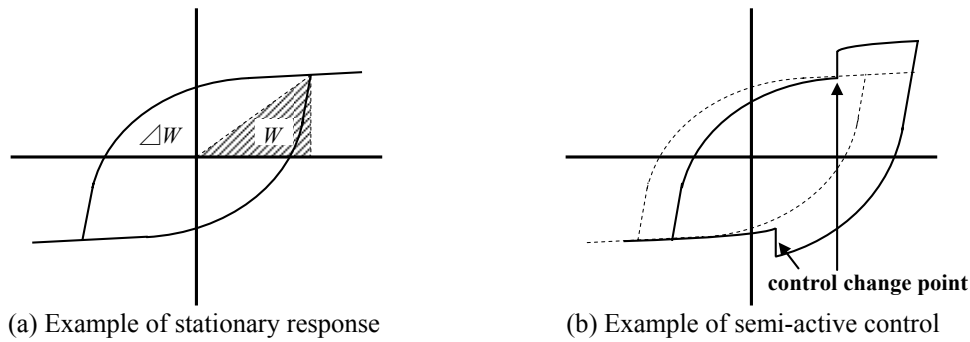


Fig.1 Concept of equivalent viscous damping factor

2.2. Proposal for a simplified quantification approach using a variable hydraulic damper

In semi-active control, the hysteresis shape of a damper changes rapidly. Therefore, a quantitative evaluation using equivalent cycle was conducted in place of an evaluation method using equivalent damping. The equivalent cycle (N_v) is a calculated index, which is obtained by dividing the amount of hysteresis energy and accumulated by a damper (E_d) during earthquake by the area per hysteresis loop cycle of a damper (E_v) in a constant amplitude sine wave calculated using the maximum relative displacement and the maximum relative velocity of the structure that was induced by the earthquake ground motion.

$$N_v = \frac{E_d}{E_v} \quad (2.2)$$

In order to obtain E_v , it is necessary to determine the parameters of a constant amplitude sine wave using the maximum relative displacement and the maximum relative velocity of the structure. The parameter of the target sine wave (frequency) can be obtained by the following Eq.2.3, and then the area per hysteresis loop cycle can be calculated based on the mechanical model of a damper with the amplitude and frequency. Here, f is the frequency of the target sine wave, V_{max} is the maximum relative velocity and D_{max} is the maximum relative displacement.

$$f = \frac{V_{max}}{2\pi \times D_{max}} \quad (2.3)$$

So, the method in this paper employs a similar equation. The corresponding relation between the maximum response of a structure at the time of an earthquake and the energy absorption performance

of a damper is used for the quantification. However, using only the equivalent cycle N_v obtained from the maximum relative velocity of a structure is likely to lead to an excessive evaluation. Therefore, the equivalent cycle N_t is obtained using the maximum relative displacement and the primary natural frequency of a structure and the average of N_v and N_t is employed as the equivalent cycle (N).

$$N = \frac{N_v + N_t}{2} \quad (2.4)$$

In accordance with the above-described procedure, this method can be applied to ordinary passive-type dampers. However, in the case of variable hydraulic dampers, the hysteresis loop of the dampers changes with various damping ranges according to the control law being employed, so the area per hysteresis loop cycle may also change considerably, depending on the damping characteristics of the damping range. Therefore, by sampling the length of time for each damping range during the earthquake, the ratio between the time and the total duration of the earthquake motion can be calculated. Based on the calculated ratios, the area per hysteresis loop cycle of a damper was apportioned between the ranges.

Fig.2 shows a flow chart of the simplified quantification approach proposed in this paper.

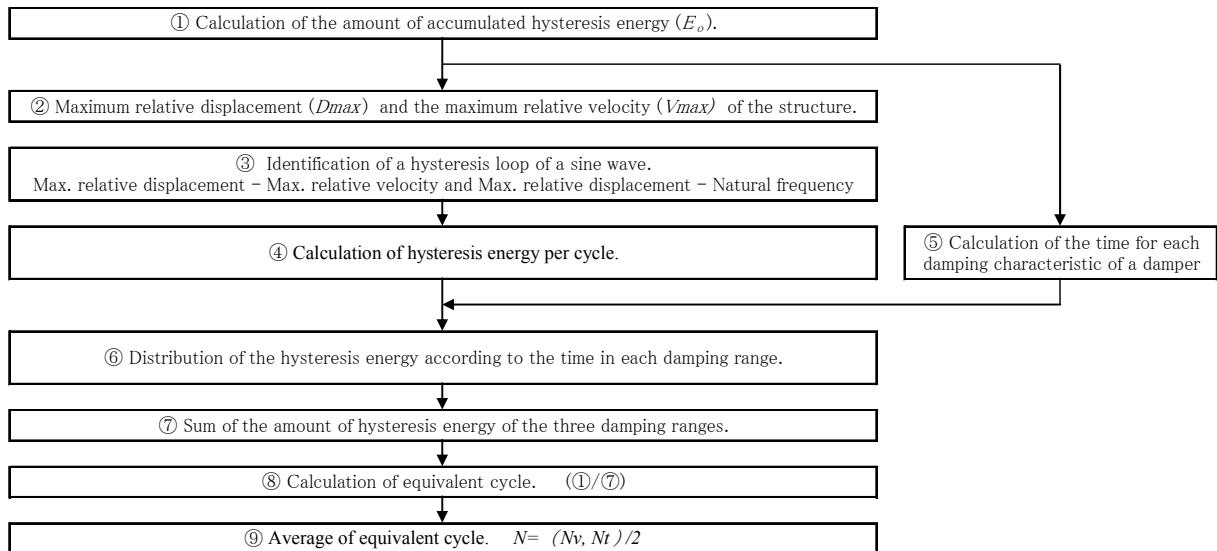


Fig.2 Flow chart of the simplified quantification approach

3. VERIFICATION OF THE SIMPLIFIED QUANTIFICATION APPROACH USING A SHAKING TABLE TEST

3.1. Characteristics of a variable hydraulic damper and its analytical model

The validity of the simplified quantification approach was verified by conducting a shaking table test using a semi-active damper and applying this simplified quantification approach to the test results. The semi-active damper used in the test was a variable hydraulic damper whose damping performance can be switched into three different ranges (C1L, C1M, C1H). A schematic of the variable hydraulic damper's structure is shown in Fig.3, and hydraulic-circuit is shown in Fig.4. Variable hydraulic damper has a hydraulic valve and two control valves in the path which connects a cylinder room on both sides. The damping force is changed by closing motion of this control valve. Table 1 shows the designs of the variable hydraulic damper. Fig.5 shows an example of the hysteresis loop under excitation of the sine wave, and Fig.6 shows the relation between the maximum velocity of the piston and the damper force. A performance curve at the time a damper is being designed. The test results show a slightly smaller value of damper force than the design value in the area where velocity was

large. However, in general, the performance satisfies the design value. It is clear from the figure that the velocity of vibration, as well as the operation of a flow control voltage valve, greatly affects the variable hydraulic damper force.

Table 1 Design of damper

Maximum Force	15 kN
Relief Force	7 kN
Stroke	± 300 mm
Cylinder Bore	φ 95 mm
Piston Rod Bore	φ 35 mm
Flow Control Valve	Solenoid Valve × 2
Control Voltage	DC 5V
Fluid	Purification mineral oil

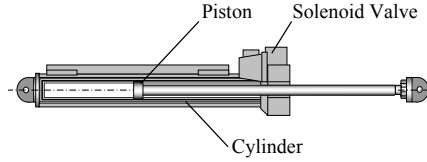


Fig.3 Variable hydraulic damper

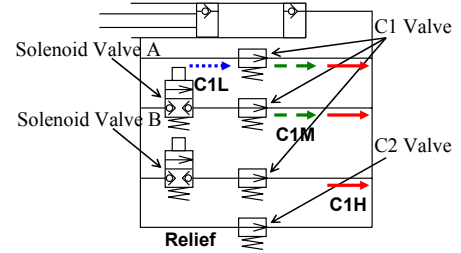


Fig.4 Hydraulic-circuit

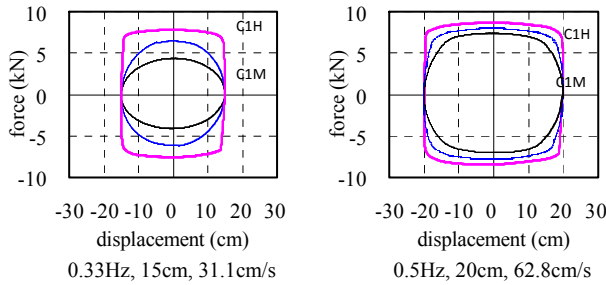


Fig.5 Force-displacement relationship

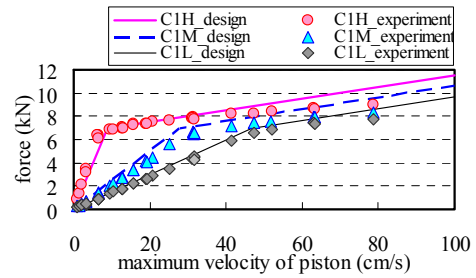


Fig.6 Force-velocity relationship

Based on the results of the dynamic loading tests, the analytical model of the variable hydraulic damper was set as a simple model of collinear approximation before and after relieving the damping force. The comparison of the test results with the analytical model shown in Fig.7 confirmed they were in close agreement. Using the damper force (F) and the damper piston velocity (\dot{x}), parameters in the three ranges of damping performance can be obtained from the following Eq.3.1-3.6.

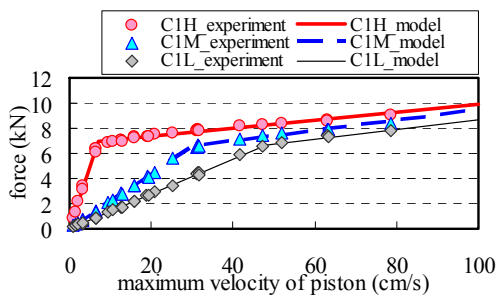


Fig.7 Comparison of test result and model

$$\begin{aligned}
 \text{【C1H】} \quad & 0 < \dot{x} \leq 7.0, \quad F = 0.99 \dot{x} \quad (3.1) \\
 & \dot{x} > 7.0, \quad F = 0.04 \dot{x} + 6.73 \quad (3.2) \\
 \text{【C1M】} \quad & 0 < \dot{x} \leq 30.1, \quad F = 0.22 \dot{x} \quad (3.3) \\
 & \dot{x} > 30.1, \quad F = 0.04 \dot{x} + 5.33 \quad (3.4) \\
 \text{【C1L】} \quad & 0 < \dot{x} \leq 48.0, \quad F = 0.14 \dot{x} \quad (3.5) \\
 & \dot{x} > 48.0, \quad F = 0.04 \dot{x} + 4.85 \quad (3.6)
 \end{aligned}$$

※ \dot{x} : piston velocity of damper

3.2. Overview of the shaking table test

A shaking table test was conducted using a two-degree of freedom system specimen that simulated the base-isolated structure (Fig.8). Base-isolated system is constituted of with two natural rubber bearings and four roller bearings in base-isolated layer. The natural rubber bearings served as restoring materials, and the roller bearings were used to support the vertical load. A variable hydraulic damper was installed on the base-isolated layer. The superstructure of the specimen was two-degree of freedom system, as the section of mass was divided into two layers by the rubber bearings. Table 2 shows characteristics of the specimen. The natural period ($T=3.43\text{sec.}$) of the base-isolated structure.

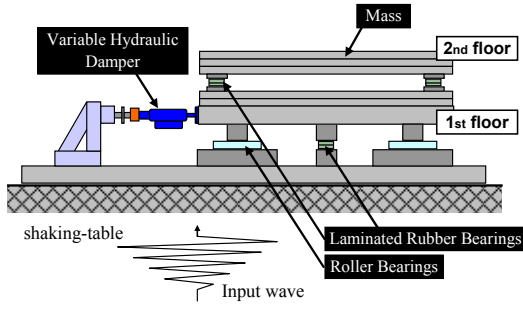


Fig.8 Specimen of the base-isolated structure

Table 2 Characteristics of specimen

Base-isolated layer		
Mass / Weight	6.3	ton
Stiffness of laminated rubber bearing	0.5	kN/cm
Damping coefficient	0.03	kN·s/cm
Friction force of roller bearing	0.29	kN
Natural period	3.43	sec
2nd floor		
Mass / Weight	8.1	ton
Stiffness of laminated rubber bearing	3.5	kN/cm
Damping coefficient	0.03	kN·s/cm
Natural period	0.95	sec

The shaking table test was conducted using a medium-sized shaking table owned by the Building Research Institute. Using a magnetic-type displacement transducer ($\pm 500\text{mm}$) in a measurement frame installed on the shaking table, the relative displacement of the specimen was measured. The acceleration data were collected using a servo-type accelerometer installed on each part of the specimen. The damper displacement was measured by an inductance-type displacement transducer installed between a piston and a cylinder, and the damper force was measured by a load-cell ($\pm 50\text{kN}$). Control signals from a sensor were diverted in a separate system from a measurement conductor, and DSP was used for the control calculations. *Matlab* and *Simulink* software were used to control the system. The damper was controlled by the 1kHz sampling command.

The control algorithm based on the LQR (*Linear Quadratic Regulator*) control theory was adopted as the semi-active control law. While keeping the absolute acceleration at a similar level with the case of a passive damper, the semi-active damper was controlled to reduce the relative displacement. The equation of motion of the two-degree of freedom system specimen is given as follows.

$$\begin{cases} m_1\ddot{x}_1 + c_1\dot{x}_1 + c_2(\dot{x}_1 - \dot{x}_2) + k_1x_1 + k_2(x_1 - x_2) + p + F = -m_1\ddot{z} \\ m_2\ddot{x}_2 + c_2(\dot{x}_2 - \dot{x}_1) + k_2(x_2 - x_1) = -m_2\ddot{z} \end{cases} \quad (3.7)$$

Where, m :mass; c :damping coefficient; k :stiffness of rubber bearings; p :frictional force of roller bearings; F :damping force by MR damper; \ddot{x} :acceleration; \dot{x} :velocity; x :displacement; \ddot{z} :acceleration of ground motion. Subscripts refer to the first layer and the second layer, respectively.

Fig.9 shows the relation between the control index and the control force. Here, J_v is the vibration energy of the structure, and J_c is the external energy required for control. As shown in the figure, if the vibration energy J_v is decreased in order to increase response control, the control force becomes larger, increasing the control energy J_c . A demand for decreasing vibration energy conflicts with a demand for decreasing control energy. However, given the sum of energy $J = (J_v + J_c)$, there exists an optimal control force u to minimize J .

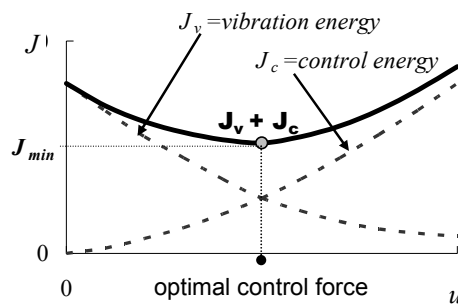


Fig.9 Relation between control index and control force

In order to comply with the control objective in this study, the evaluation function (J) and the control force (F) are determined in the following equations.

$$J = \int_0^{\infty} \{ \alpha_1 (\ddot{x}_1 + \ddot{z}) + \alpha_2 (\ddot{x}_2 + \ddot{z}) + \beta x_1^2 + \gamma u^2 \} dt \quad (3.8)$$

$$\begin{cases} F = \text{sgn}(\dot{x}_1) u \\ u = \{f_1, f_2, f_3, f_4\} \{x_1, \dot{x}_1, x_2, \dot{x}_2\}^T \end{cases} \quad (3.9)$$

Based on the above, feedback vectors $\{f_1, f_2, f_3, f_4\}$ were determined, where J became the smallest. The control force of a semi-active damper can exert resistance force only in the opposite direction of the relative velocity of the base-isolated layer, so the following limits are given to the damping force F actually occurring in a variable hydraulic damper.

3.3. Test results and simulation

Input waves used in the shaking table test were the observed second seismic wave (El Centro(1940)NS, Hachinohe(1968)NS), with the input levels of the original wave and the wave determined by standardizing the maximum velocity at 25 cm/s. There is a trade-off relation in the base-isolated structure: when damping in the base-isolated layer becomes larger to control displacement, acceleration response in the superstructure will increase (Fig.10).

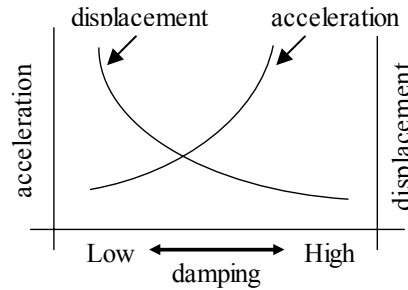


Fig.10 Relation between displacement and acceleration

Fig.11 shows the relation between the maximum relative displacement and the maximum acceleration of each input wave in the base-isolated layer (on the left-side) and the second layer (on the right-side). The test results are for two cases: the non-control case, where the excitation was given in three damping ranges without controlling a damping performance, and the control case, where the semi-active control was conducted by applying the LQR control theory. The analytical results (damping changes) of simulation are also presented in the figure.

In the simulation, damping constants of the specimen were changed under the condition without a damper, using the following damping constants: $h=0.01, 0.03, 0.05, 0.10, 0.15, 0.20, 0.25, 0.30, 0.50$. The damping matrix was calculated in the proportional damped system.

The test results show that by increasing the damping of a damper from C1L to C1H, displacement of the base-isolated layer could be controlled, and there was an increase in acceleration. The response of the second layer shows that displacement and acceleration tended to increase due to the effect of the acceleration in the base-isolated layer, when damping in the base-isolated layer was large. It can be confirmed from the results of the semi-active control that displacement and acceleration in the base-isolated layer were controlled, and particularly in the second layer, the response could be reduced considerably due to the control effect. The analytical results when damping constants of the specimen were changed under the condition without a damper and the test results under non-control follow almost the same locus. However, in the case of C1H where the damping performance of a variable hydraulic damper was high, the strong nonlinearity after the relief was recognized as being a remarkable characteristic. Therefore, it can be confirmed that the loci of response results were significantly different from those of analytical results when damping constants were changed.

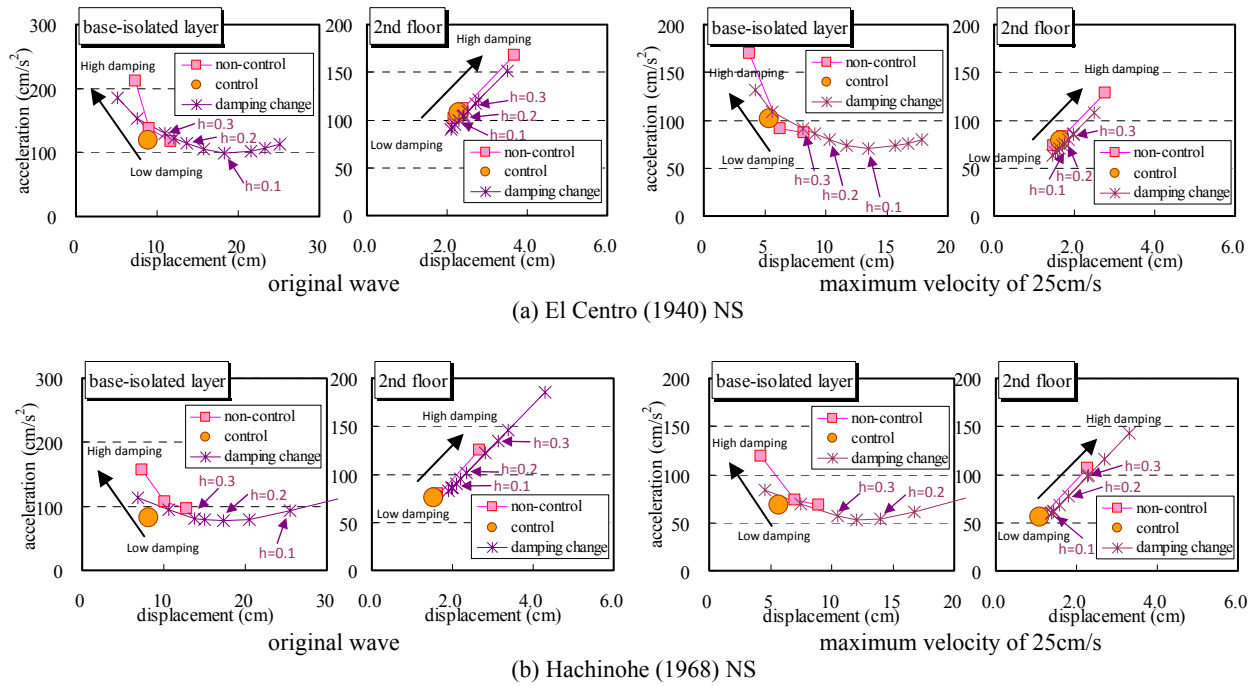


Fig.11 Experimental results of the shaking table test

3.4. Application of a simplified quantification approach

An attempt was made to apply a simplified quantification approach to the results of the shaking table tests. The following investigations were conducted according to the procedures (① to ⑨) in the flow chart shown in Fig.2. In the examples, the input earthquake was assumed to be the original wave of El Centro(1940)NS, and this method was applied to the semi-active control (LQR) and the three non-control (C1L, C1M, C1H) cases.

①. Calculation of the amount of accumulated hysteresis energy

Fig.12 shows a time history of accumulated hysteresis energy by a damper during earthquake. When the damper was not controlled (the non-control case), the amount of accumulated hysteresis energy increased as the range was switched from C1L to C1H. In the semi-active control, the amount was between C1L and C1M. Comparison with the response results of the specimen shown in Fig.11 confirmed that the small hysteresis energy could decrease response. That is, energy could be absorbed efficiently.

②. Maximum relative displacement and the maximum relative velocity of the structure

Table 3 shows the maximum relative displacement and relative velocity of the base-isolated layer, in the control (LQR) and non-control (C1L, C1M, C1H) cases. It also shows the excitation frequency of the sine wave obtained from the maximum relative displacement and relative velocity. The excitation frequency of the target sine wave was calculated from Eq.3.9 above.

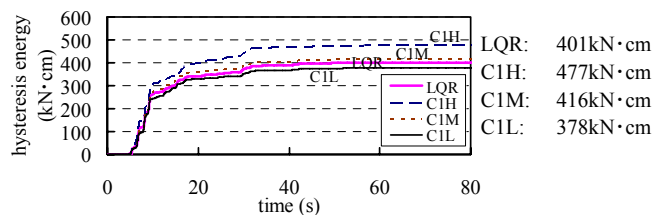


Fig.12 The hysteresis energy during earthquake

Table 3 Frequency of target sine wave

	Max. relative displacement (cm)	Max. relative velocity (cm/s)	Frequency of target sine wave (Hz)
LQR	8.42	31.9	0.60
C1H	7.32	33.3	0.72
C1M	9.02	38.9	0.69
C1L	11.7	44.3	0.60

③,④. Identification of a hysteresis loop of a sine wave and hysteresis energy per cycle

Based on the results of ②, a hysteresis loop of the sine wave of a damper in each test case was identified using the analytical model described in 3.1. The loops are shown in Fig.13. The amount of hysteresis energy per cycle was also calculated. In the semi-active control, the damping range was set to one of three levels according to its control law, in order to calculate the amount of hysteresis energy per cycle for each hysteresis loop.

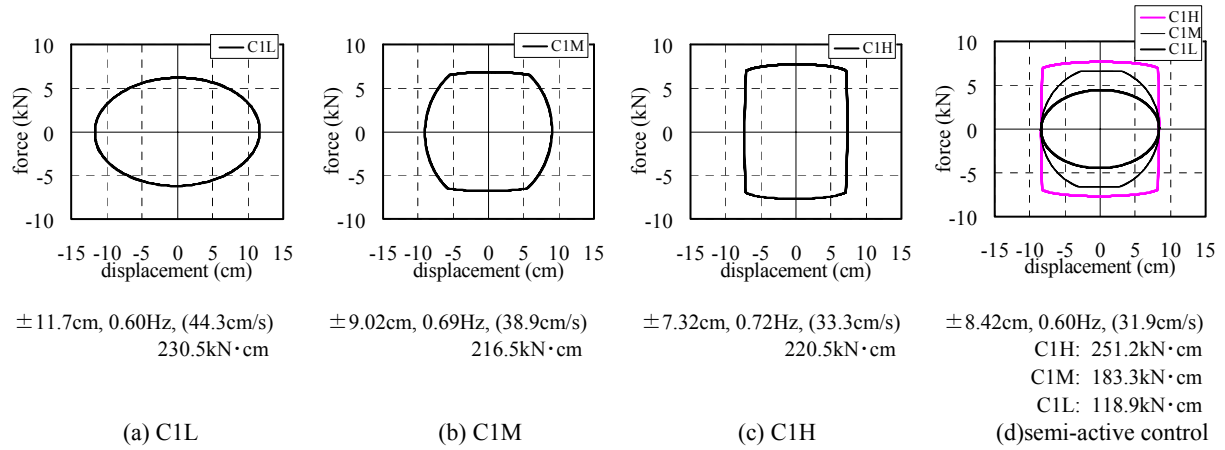


Fig.13 Identified hysteresis sine wave of a damper and the amount of hysteresis energy

⑤. Calculation of the time for each damping characteristic of a damper

A variable hydraulic damper switches the damping range into one of three levels by the semi-active control law, thereby switching each damping characteristic. Based on the measured data, the proportion of the time for each damping range was determined during the earthquake. The total duration of earthquake was 88.00 sec., which was divided into 75.29 sec. for C1L, 11.84 sec. for C1M, and 0.87 sec. for C1H.

⑥. Distribution of the hysteresis energy according to the time in each damping range

The hysteresis energy per cycle obtained from the hysteresis loop of the target sine wave (Fig.13(d)) was distributed based on the proportion of the time duration for each damping range determined in ⑤. The results of the calculations are shown below.

$$\begin{aligned}
 \text{C1L} &: 118.9\text{kN}\cdot\text{cm} \times 75.29\text{sec.} / 88\text{sec.} = 101.7\text{kN}\cdot\text{cm} \\
 \text{C1M} &: 183.3\text{kN}\cdot\text{cm} \times 11.84\text{sec.} / 88\text{sec.} = 24.7\text{kN}\cdot\text{cm} \\
 \text{C1H} &: 251.2\text{kN}\cdot\text{cm} \times 0.87\text{sec.} / 88\text{sec.} = 2.5\text{kN}\cdot\text{cm}
 \end{aligned}$$

In the non-control case, because the damping range was constant during the earthquake, the proportion in each range was 88 sec/88 sec. = 1.0. Therefore, the area of one cycle of a hysteresis loop of a sine wave simply equaled the amount of the hysteresis energy.

⑦. Sum of the amount of hysteresis energy of the three damping ranges

The total amount of hysteresis energy in each damping range obtained in ⑥ was calculated. The sum of the hysteresis energy equivalent to one cycle of a hysteresis loop of a sine wave under the semi-active control was $\Sigma = (101.7 + 24.7 + 2.5) = 128.9 \text{ kN}\cdot\text{cm}$; in contrast, the sum of the hysteresis energy in the non-control case (where the damping range was constant) was C1L: 230.5 kN·cm, C1M: 216.5 kN·cm, and C1H: 220.5 kN·cm.

⑧. Calculation of equivalent cycle

The equivalent cycle (N_v) based on the response value of the specimen was calculated by dividing the hysteresis energy (E_d) accumulated during the earthquake by the hysteresis energy per cycle calculated in ⑦. The value obtained for the semi-active control was $401\text{kN}\cdot\text{cm} / 128.9\text{kN}\cdot\text{cm} = 3.11$

cycles. Table 4 shows the calculated equivalent cycle in the semi-active control and non-control cases.

Table 4 Equivalent cycle (N_v) based on relationship between maximum relative displacement and maximum relative velocity

	Ammounted hysteresis energy (E_d) (kN·cm)	Hysteresis energy of per cycle (E_v) (kN·cm)	Equivalent cycle (N_v) E_d / E_v
LQR	401	128.9	3.11
C1H	477	220.5	2.16
C1M	416	216.5	1.92
C1L	378	230.5	1.64

⑨. Average of equivalent cycle

Using the same procedure from ③ to ⑧, the hysteresis loop of a sine wave was defined by the maximum relative displacement and the primary natural frequency, to calculate the equivalent cycle (N_t). Table 5 shows N_v , N_t , and the average equivalent cycle (N).

Table 5 average of equivalent cycle

	Equivalent cycle (N_v) (Max. velocity)	Equivalent cycle (N_t) (Natural frequency)	Average of equivalent cycle (N) $(N_v + N_t) / 2$
LQR	3.11	3.27	3.19
C1H	2.16	2.40	2.28
C1M	1.92	4.00	2.96
C1L	1.64	3.40	2.52

Fig.14 shows the relation between maximum displacement of base-isolated layer and the average equivalent cycle of each input wave. For comparison, the figure also shows the equivalent cycles in the non-control cases that were calculated using this method.

The equivalent cycle in the semi-active control was larger than in the non-control in every case. This shows that due to the control effect, the equivalent cycle for the area of the hysteresis loop of the target sine wave increased, and the damper absorbed a greater amount of energy. The equivalent cycle in the non-control case increased in the order of C1H < C1L < C1M. The largest cycle was confirmed in C1M.

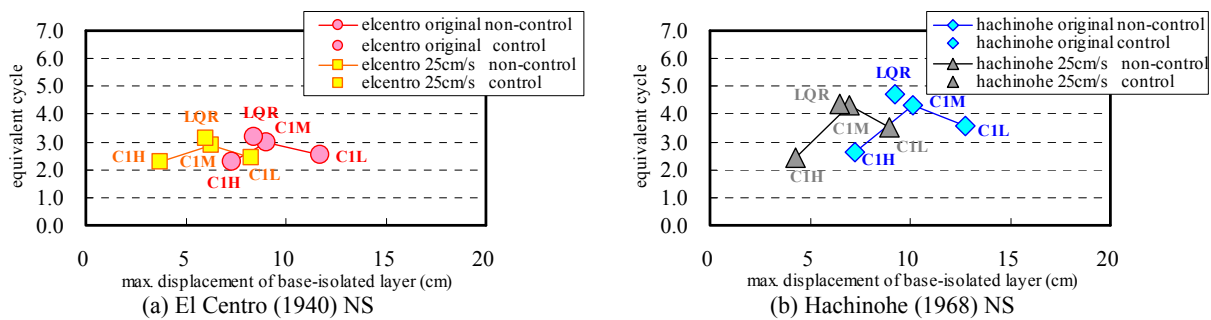


Fig.14 Relation between maximum displacement of base-isolated layer and equivalent cycle

3.5. Verification of calculated results by the simplified quantification approach

In order to confirm the validity of this method, the relation between the response and the equivalent cycle of the specimen was verified. The displacement obtained from the test was divided by the maximum displacement in the base-isolated layer, and the acceleration was divided by the maximum input acceleration of the earthquake, thus making responses dimensionless, as shown in Fig.15.

It is desirable for both the response displacement and the acceleration of a structure to decrease. That is, when the distance from the original point in the figure is shorter, the effect of reducing the response is stronger. Fig.15 also shows the calculated distance from the original point for each test result.

The calculated distances from the original point showed a marked tendency (i.e. the shortest distance)

in the control case. On the other hand, in the non-control case, the value decreased in the order of C1M–C1L–C1H. Also, the equivalent cycle calculated using a simplified quantification approach decreased in the order of LQR–C1M–C1L–C1H. This confirmed that the damping performance of a damper can be quantified using the equivalent cycle corresponding to the response value of the structure and the damping performance of the damper.

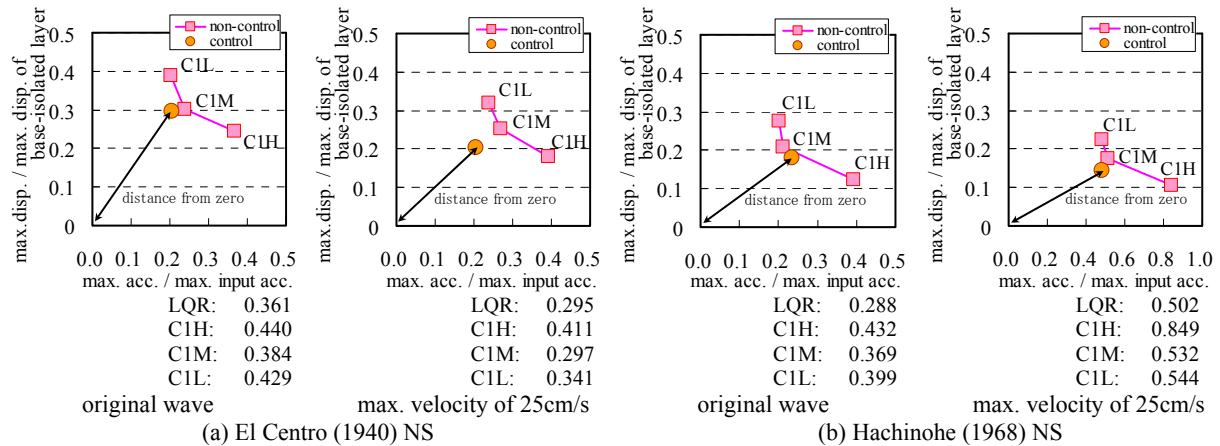


Fig.15 Verification of the response results

4. CONCLUSIONS

In order to determine the damping performance of a variable hydraulic damper under semi-active control, this paper examined a simplified quantification approach using the equivalent cycle, which has a corresponding relation with response values of the structure. Moreover, this method was applied to the results of a shaking table tests to verify its validity. As a result, it was confirmed that a damper could become more effective as the equivalent cycle increased by applying semi-active control to the damper based on the responses of the structure. In this method, the hysteresis properties of a damper were calculated in a simplified manner without using complicated equations. A previous study had proposed evaluation equations for a hydraulic damper with a relief mechanism, in order to obtain an exact solution for the amount of hysteresis energy, by taking into account detailed mechanical properties of the damper (rigidity element, bi-linear characteristic, etc.). Future studies should focus on the differences between such evaluation methods and the quantification method proposed in this paper.

ACKNOWLEDGEMENT

In this study, a medium-sized shaking table owned by the Building Research Institute was used. The author would like to express his appreciation to Dr. Taiki Saito, and Mr. Namihiko Inoue, at the Building Research Institute, for their kind assistance. This study was financially supported by the Hyogo COE Program Promotion Project (2004-2005) and the Maeda Memorial Engineering Promotion Foundation (2006). The author wishes to express his gratitude to the parties concerned. The author is also grateful to Dr. Kenichi Oi and the parties concerned for letting him use the variable hydraulic damper for the test, which had been originally made during the “Development of Seismic Renewal Technology by Energy Dissipation-Type Movable Juncture of Structures” that was conducted under a Basic Study for Scientific Research Grant (B) (2005-2006)

REFERENCES

- L.S.Jacobsen. (1960). Damping in Composite Structure. *Proceedings of 2nd WCEE*. vol.2. : 1029-1044.
- Yang, J.N. (1975). Application of Optimal Control Theory to Civil Engineering Structure. *Journal of The Engineering Mechanics Division*. : 819-838.
- MATLAB® : The MathWorks, Inc., Natick, Mass.
- SIMULINK® : The Math Works, Inc., Natick, Mass.